AIP Journal of Applied Physics

# Electronic structure and electrical transport properties of LaCo1xNixO3 (0x0.5)

Vinod Kumar, Rajesh Kumar, D. K. Shukla, Sanjeev Gautam, Keun Hwa Chae, and Ravi Kumar

Citation: Journal of Applied Physics **114**, 073704 (2013); doi: 10.1063/1.4818448
View online: http://dx.doi.org/10.1063/1.4818448
View Table of Contents: http://scitation.aip.org/content/aip/journal/jap/114/7?ver=pdfcov
Published by the AIP Publishing

JOURNAL OF APPLIED PHYSICS 114, 073704 (2013)

# Electronic structure and electrical transport properties of $LaCo_{1-x}Ni_xO_3$ ($0 \le x \le 0.5$)

Vinod Kumar,[1,a)] Rajesh Kumar,[1] D. K. Shukla,[2,b)] Sanjeev Gautam,[3] Keun Hwa Chae,[3] and Ravi Kumar[4,c)]

[1]*Department of Physics, National Institute of Technology, Hamirpur (H.P) 177 005, India*
[2]*Deutsches Elektronen-Synchrotron DESY, 22607 Hamburg, Germany*
[3]*Advanced Analysis Center, Korea Institute of Science and Technology (KIST), Seoul 136 791, South Korea*
[4]*Centre for Materials Science & Engineering, National Institute of Technology, Hamirpur (H.P) 177 005, India*

(Received 19 June 2013; accepted 30 July 2013; published online 16 August 2013)

The structural analysis of $LaCo_{1-x}Ni_xO_3$ ($0 \le x \le 0.5$) samples assures single phase rhombohedral structure with space-group $R\bar{3}c$. Electronic structure of these samples has been studied by x-ray absorption near edge spectroscopy (XANES) at K-edge of O, Ni, Co and $M_{5,4}$ edge of La. These studies confirm the trivalent state of Co/Ni and La in all the compositions. Upon substitution of the Ni at the Co site in $LaCoO_3$, the O K-edge spectra show a feature about 1.2 eV lower than that of $LaCoO_3$. This feature keeps on growing as the concentration of the Ni is increasing. This is consistent with our resistivity data which shows drastic decrease in resistivity with the Ni substitution. The resistivity data have been analyzed using Arrhenius and Efros-Shklovski's type variable range hopping models in different temperature ranges. The activation energy decreases and localization length increases systematically with increase in the Ni concentration. Observed features have been explained on the basis of change in charge-carrier density with substitution. The disorder-induced localization of carriers is found to govern conduction mechanism and resistivity behavior in substituted sample. © *2013 AIP Publishing LLC*. [http://dx.doi.org/10.1063/1.4818448]

## I. INTRODUCTION

Perovskite transition metal oxides with the general formula $RMO_3$ ($R$ = Rare earth, M = Transition metals) have been of much interest for more than five decades. The interplay between onsite and inter-site coulomb interaction, the charge transfer energy, hybridization strength between cation $3d$ & oxygen $2p$ states, and crystal field splitting control the transport and magnetic properties of these perovskites. Among $LaMO_3$ compounds (M = Ti, V, Cr, Mn, Fe, Ni) which are well known as strongly correlated systems, $LaCoO_3$ has been extensively studied; it exhibits the characteristic behaviour associated with the metal–insulator transition (MIT) as well as with magnetic properties due to a change in the spin state of the Co ion.[1–7]

This spin state transition and properties can be controlled by substitution either at the La or Co cation sites. $LaCoO_3$ has already been reported by introducing different cations both in the La (e.g., $Sr^{2+}$, $Ca^{2+}$) and Co (e.g., $Mg^{2+}$) perovskite sublattices.[8–10] These studies clearly show that such heterovalent substitution leads to the formation of hole states as well as creates $Co^{4+}$ ions, leading to ferromagnetism and insulator to metal (IM) transitions. Dho *et al.*,[11] studied $LaMO_3$ with doping at M site with various transition metals and conclude that the Ni ion plays a significant role in deciding the behavior of electrical transport.

$LaNiO_3$ is a paramagnetic metallic oxide. The $Ni^{+3}$ is in low spin state ($t^6_{2g}$, $e^1_g$) and the conduction band is formed by the hybridization of the $Ni^{+3}$ $e_g$ orbitals and $O^{-2}$ $2p$ orbitals.[12] $LaCoO_3$ is a nonmagnetic insulator at low temperature and exhibit spin state dependent properties at high temperature as described above. $LaCo_{1-x}Ni_xO_3$ has attracted considerable attention from researchers due to the presence of the glassy ferromagnetism, magneto resistance, and MIT in this system.[13,14] In the previous studies on $LaCo_{1-x}Ni_xO_3$, the results have been explained on the basis of assumption of charge disproportion, but without any evidence regarding electronic structure.[13–16] However, Wu *et al.*[17] performed photoemission study and provides two band model for the $LaCo_{1-x}Ni_xO_3$ series. Also in our recent finding on $NdCo_{1-x}Ni_xO_3$, we have ruled out any charge disproportion in these systems and homovalent substitution was confirmed through x-ray absorption results.[18] So it will be interesting to study the effect of homovalent substitution ($Co^{+3}$ by $Ni^{+3}$), as this makes the system ideally suited for investigating possible manifestations of disorder effects within the strongly interacting transition metal oxide system. This is further evident from the electronic structure investigations probed with the help of X-ray absorption spectroscopy (XAS) at the O K-edge on homovalent substituted $LaNi_{1-x}M_xO_3$ (M = Mn, Fe, and Co) and $LaFeNiO_3$ systems.[19,20] In these investigations, potential mismatch between the substituent metal ion and the host ion has been suggested to cause disorder and change in the density of states near the $E_F$ (Fermi level) leading to changes in the transport properties. So in the present paper, we have investigated the crystallographic structure and electrical transport

a)Electronic mail: kumarvinodphy@gmail.com
b)Present address: UGC DAE Consortium for Scientific Research, Indore 452 001, India.
c)Present address: BCET, Gurdaspur, Punjab 143 521, India.

 

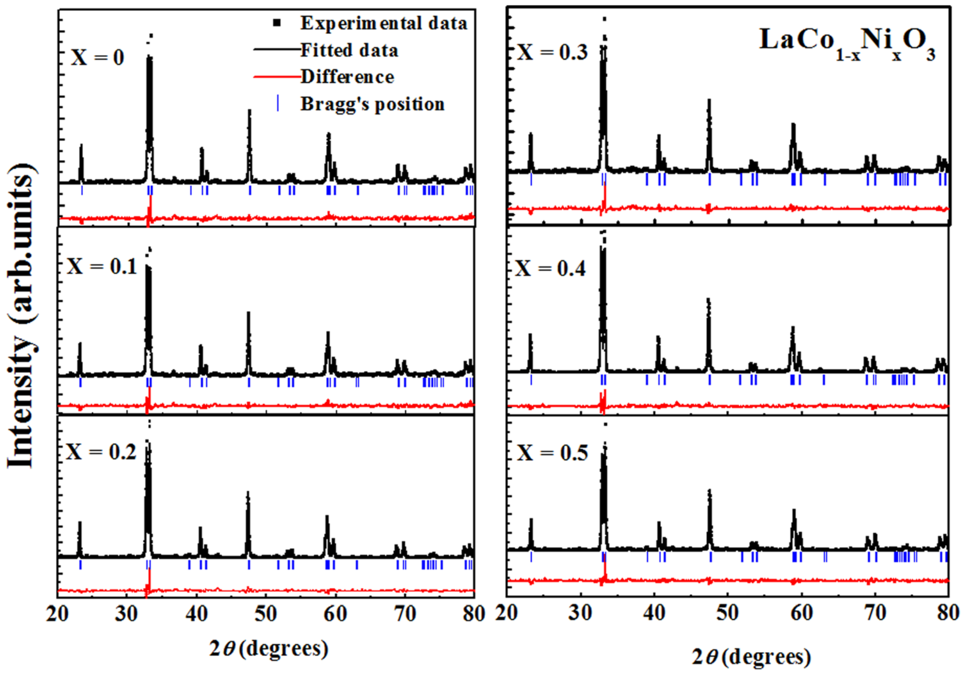


FIG. 1. Reitveld refined X-ray diffraction patterns for the samples $LaCo_{1-x}Ni_xO_3$ ($0 \leq x \leq 0.5$). In each panel, solid squares represent observed data; the line shows the calculated profile. The difference between the observed and the calculated pattern is shown at the bottom.

properties of $LaCo_{1-x}Ni_xO_3$. In order to put emphasis on understanding of its electronic properties and electronic structure, the effect of Ni substitution at Co site has been explored through the x-ray absorption near edge spectroscopy (XANES) at O K-edge along with XANES measurements at Co/Ni K-edge.

## II. EXPERIMENT DETAILS

Polycrystalline $LaCo_{1-x}Ni_xO_3$ perovskite oxides ($x = 0.0$–$0.5$), were prepared using the conventional solid-state reaction method. Required stoichiometric amounts of $La_2O_3$, $Co_2O_3$, and NiO were thoroughly mixed, ground, and heat treated in air at 900 °C with intermediate grinding. The resulting materials were ground and pressed into pellets. These pellets were finally sintered at 1200 °C. In all treatments, the heating as well as cooling rate was maintained at 3 °C $min^{-1}$. The crystal structure of the sintered samples was characterized by x-ray diffraction using PANanalytical X′PertPRO, x-ray diffractometer having Cu K$\alpha$ ($\lambda = 1.5418$ Å) radiation source. The resistivity measurements were performed using a conventional four-probe technique in the range of 85–300 K. X- ray absorption studies at K-edges of Co and Ni have been performed at C beam line of the DORIS III storage ring (DESY, Hamburg, Germany) at 77 K. Spectra at Ni K-edge were collected in fluorescence and transmission mode both, while that for Co was collected only in transmission mode. The XANES spectra at *O* K-edge and *La* $M_{5,4}$ edge of these materials were obtained using 10D XAS-KIST (X-ray absorption spectroscopy- Korea Institute of Science and Technology) bending magnetic beam-line of Pohang Accelerator Laboratory (PAL). All measurements were processed in an ultra-high vacuum chamber ($10^{-9}$ Torr) at 300 K in total electron yield (TEY) mode. After a constant background subtraction, all spectra were normalized to the post-edge step height using Athena 0.0.061.[21]

## III. RESULTS AND DISCUSSION

### A. X-ray diffraction (XRD)

Figure 1 shows the XRD patterns of the $LaCo_{1-x}Ni_xO_3$ ($0 \leq x \leq 0.5$) series. The Rietveld analysis confirms the single phase rhombohedral structure and $R\bar{3}c$ space group for all the compositions. In $LaCo_{1-x}Ni_xO_3$, La is associated with Wyckoff position 6*a* (0, 0, 1/4), Co is at position 6*b* (0, 0, 0) and O is at 18*e* (x, 0, 1/4). The unit cell parameters found to increase with the nickel substitution (see Table I), which is consistent with the difference in the ionic radii as r ($Ni^{+2}$) > ($Ni^{+3}$) > r ($Co^{+3}$).[17] A schematic view of LaCo(Ni)$O_3$ unit cell is presented in Fig. 2, which shows the various atomic positions of this compound.

### B. Electrical resistivity

To determine the effect of substitution on conduction mechanism, temperature dependent *dc* resistivity was measured in the temperature range of 85–300 K for $LaCo_{1-x}Ni_xO_3$ ($0 \leq x \leq 0.5$), as presented in Fig. 3(a). Temperature dependence of resistivity, $\rho(T)$, shows semiconducting behavior, in the

TABLE I. Unit cell and electrical transport parameters for $LaCo_{1-x}Ni_xO_3$ ($0 \leq x \leq 0.5$) samples.

| Name | $a$ (Å) | $c$ (Å) | $\chi^2$ | $E_a$ (eV) | $T_{0\,(ES)} \times 10^3$ (K) |
|---|---|---|---|---|---|
| $LaCoO_3$ | 5.4441 | 13.097 | 1.38 | 0.12 | 142.9 |
| $LaCo_{0.9}Ni_{0.1}O_3$ | 5.4489 | 13.105 | 2.14 | 0.06 | 28 |
| $LaCo_{0.8}Ni_{0.2}O_3$ | 5.4545 | 13.111 | 1.96 | … | 15.89 |
| $LaCo_{0.7}Ni_{0.3}O_3$ | 5.4605 | 13.122 | 2.15 | … | 12.09 |
| $LaCo_{0.6}Ni_{0.4}O_3$ | 5.4620 | 13.124 | 2.03 | … | 4.739 |
| $LaCo_{0.5}Ni_{0.5}O_3$ | 5.4700 | 13.143 | 1.02 | … | 0.724 |

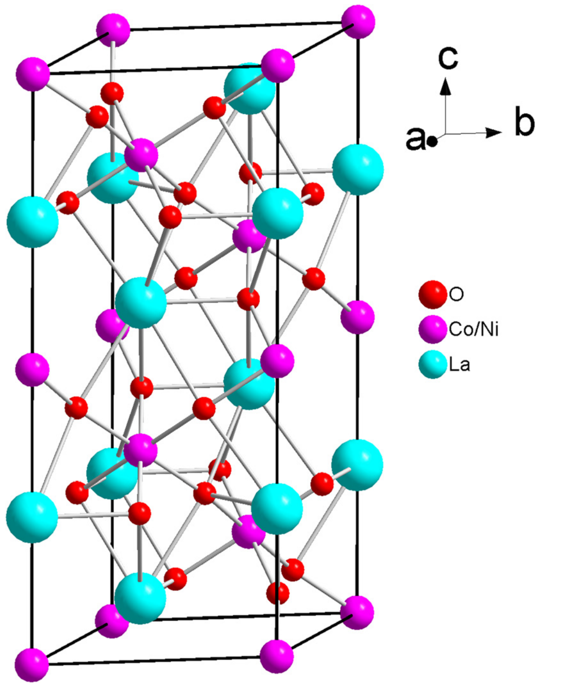


FIG. 2. Schematic presentation of $LaCo(Ni)O_3$ unit cell.

whole temperature and composition range. It is observed that the resistivity decreases with increase in the Ni substitution. Room temperature resistivity is observed to reduce from 2.28 Ω cm for x = 0 to 0.01 Ω cm for x = 0.5. The resistivity data were fitted using Arrhenius law as well as variable range hopping (VRH) model. Former with $\rho = \rho_o \exp(E_a/kT)$ describes thermally activated behavior due to the presence of energy gap $E_a$, whereas later with $\rho = \rho_o \exp[(T_0/T)^s]$, where $\rho_o$ being pre exponential factor and $T_0$ as characteristic temperature coefficient, describes variable range hopping of conduction mechanism. The exponent's depends critically on the nature of hopping process and is equal to 1/4 for Mott's[22] and 1/2 for Efros-Shklovski's (ES) variable range hopping law.[23] It is observed in Fig. 3(b) that for $x \geq 0.1$, $\rho(T)$ curves are well

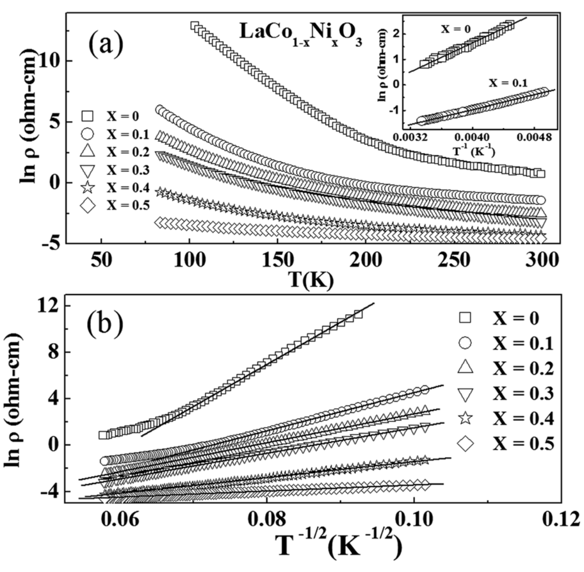


FIG. 3. (a). The electrical resistivity of $LaCo_{1-x}Ni_xO_3$ ($0 \leq x \leq 0.5$), (b) plots of ln $\rho$ *vs* $T^{-1/2}$. The inset shows a plot of ln $\rho$ vs $T^{-1}$ for x = 0 and 0.1.

described using ES hopping law, but no single law of conduction fits the entire range of temperature for pure as well as for x = 0.1. It suggests that there are two types of mechanisms which govern conduction in different temperature ranges of these samples. In high temperature range (200–300 K), for x = 0, 0.1, Arrhenius law fits well (see inset to Fig. 3(a)), while in the low temperature region (100–200 K), the conduction is governed by ES hopping. Such a change from thermal carrier activation at higher temperature to VRH at low temperatures usually occurs in disordered systems.[24]

In the octahedral crystal field as is the case in present system, Coulomb repulsion with ligands and *p*–*d* hybridization leads to the splitting of *d* levels ($t_{2g}$ and $e_g$) see Fig. 4(a). It can easily be seen that the $e_g$-orbitals have a rather large overlap and hence makes a strong hybridization with the *p*-orbitals of oxygen (directed towards the TM ion) leading to so called $\sigma$-bond. Whereas $t_{2g}$-orbitals are orthogonal to the *p*-orbitals and by symmetry the overlap of $p_\sigma$-orbitals with the $t_{2g}$-orbitals is zero and only permitted overlapping is $\pi$-hybridization, which is smaller than that of $e_g$-orbitals.[25] Hence, the band width of the $\sigma$-band is substantially larger than that of $\pi$ -band; therefore, one can consider that only the $e_g$ electrons are able to move close to the Fermi level. Consequently, for a number of perovskites, the $t_{2g}$ states are localized while the $e_g$ states form $\sigma$-conduction bands;[26] $LaNiO_3$ with filled $t_{2g}$ states and a single electron in the $e_g$ band is an example.[12] So in case of $LaCo(Ni)O_3$, the conduction band is also made up of $e_g$ electrons of Ni and Co ions, as has been described for similar system.[27]

As Ni ions are substituted for Co partly, so they are distributed at random in the lattice. Since there is a difference in the energy of 3*d* orbitals of Ni and Co, they will give rise to energy inequivalent sites distributed randomly constituting a disordered system with random potential giving rise to Anderson localization.[28,29] In such a disordered system, the density of states may still form continuous bands rather than discrete energy levels, but the states which overlap to form these band states are more likely to have neighbours with energies near the average value than those with similar energy. As a consequence, orbitals with energy close to the center of the band may be able to extend through the solid, while the lowest states near the band edges may be localized. The extent of localization depends on the degree of disorder relative to the band width. Thus in a sufficiently disordered system, a conduction band is formed which consist of an energy level called as mobility edge ($E_\mu$) which separates the localized and nonlocalized or extended energy states.[29–31] The conduction then depends on the relative position of Fermi energy level and mobility edge (see Fig. 4(b)), because the activation energy is proportional to $E_\mu - E_F$, which is further governed by concentration of carriers. The value of activation energy calculated for samples (x = 0, 0.1) is given in Table I, which decreases sharply for x = 0.1, suggesting that Ni substitution is not only increasing carrier concentration but it also decreases the band gap leading to the observed decrease in resistivity.

For samples with $x \geq 0.1$, ES hopping is found in the entire temperature range, which indicates that Ni substitution introduces sufficient disorder in the system which grows

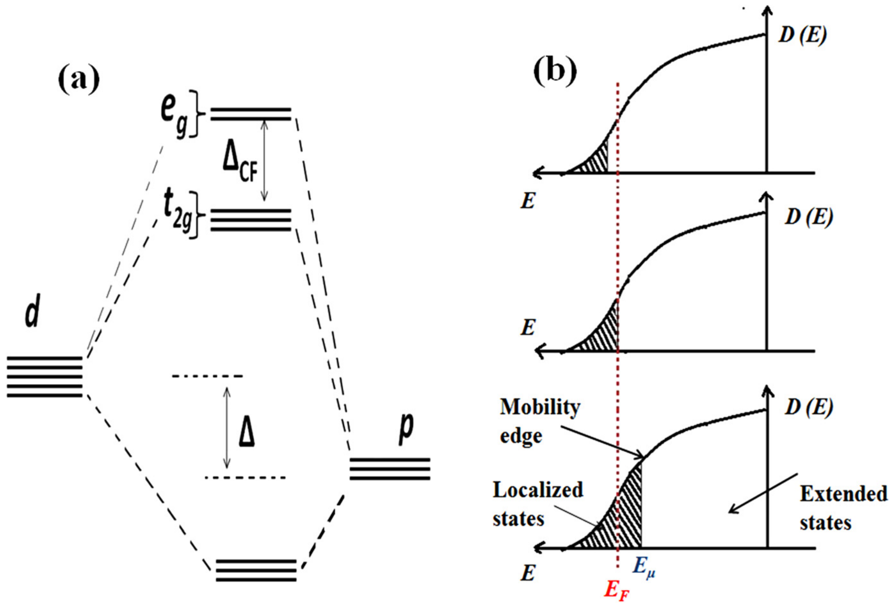


FIG. 4. (a) The hybridization of d-levels of the TM ions and p-levels of the ligand leading to the repulsion of levels and splitting of $t_{2g}$ and $e_g$-levels, (b) the system is insulating (top) as long as the Fermi energy ($E_F$) lies within the localized states (shaded regions), when the mobility edge passes the Fermi energy (centre), the system shows metallic behaviour (bottom).

with increasing substitution. We have also calculated the value of characteristic temperature coefficient $T_{0(ES)}$ (see Table I) using slope of ln $\rho$ vs $T^{-1/2}$ plots shown in Fig. 2(b). $T_{0(ES)}$ is related to dielectric constant ($\varepsilon$) and localization length ($\xi$) through equation $T_{0(ES)} = 2.8\ e^2/k\varepsilon\xi$. We find that $T_{0(ES)}$ decreases with increasing Ni concentration, which suggest that localization length increases, thereby decreasing resistivity. So, these results suggest that the conduction mechanism in these materials is controlled by disorder-induced localization of charge carriers.

### C. X-ray absorption spectroscopy

To investigate the electronic states of $LaCo_{1-x}Ni_xO_3$, we measured the x-ray absorption spectra at K edges of O, Co, and Ni. It is well known that the study of x-ray absorption spectra at O K-edge is a tool to probe the unoccupied states with the O 2*p* symmetry due to the dipole selection rules. It arises mainly due to the hybridization of 2*p* states of oxygen with 3d state of neighboring Co and Ni atoms and also the *d* state of La in the present case. Figure 5 shows the O K-edge x-ray absorption spectra of $LaCo_{1-x}Ni_xO_3$ samples. The spectrum of pure $LaCoO_3$ can be understood in different energy ranges corresponding to various excitations from O1*s* core level, because the relative order of such levels depends on the relative strength of the different metal-oxygen interactions. In this way, the features at low energy range (between 528 and 533.5 eV) correspond to transitions which occur from O 1s core level to hybridized states between Co 3*d* and O 2*p* subbands. The next energy range (between 533.5 and 540.5 eV) corresponds to hybridization between mixed La 5*d* and O 2*p* subbands, and the structure with two peaks above at highest energy range (between 540.5 and 550 eV), to hybridization between mixed Co 4*sp* and O 2*p* sub bands. All these assignments on pure $LaCoO_3$ compound are in agreement with earlier work.[5,32]

In case of Ni substituted samples, a well-established peak "a" appears at 528.3 eV, which is about 1.2 eV lower than the energy of the pre-edge peak "b" in the pure $LaCoO_3$ system. With the increase in the Ni substitution, there is a continuous increase in intensity of the peak "a" with simultaneous decrease in that of the "b," which then appears as a broad structure for x = 0.5. The spectra in higher energy region, however, remain unaltered. The new feature is close to that of reported O K edge spectra of $LaNiO_3$, which clearly indicates here the signature of $Ni^{+3}$ state as in $LaNiO_3$.[33] Similar results have been found already for the addition of Ni in $LaFeO_3$, $PrFeO_3$, and $NdFeO_3$.[19,20,34–38] The presence of this feature is due to the metallic conduction band formed by the hybridization between Ni 3*d* and O 2*p* orbitals in the host structure. This Ni character dominates with substitution, indicating the increase in this new band

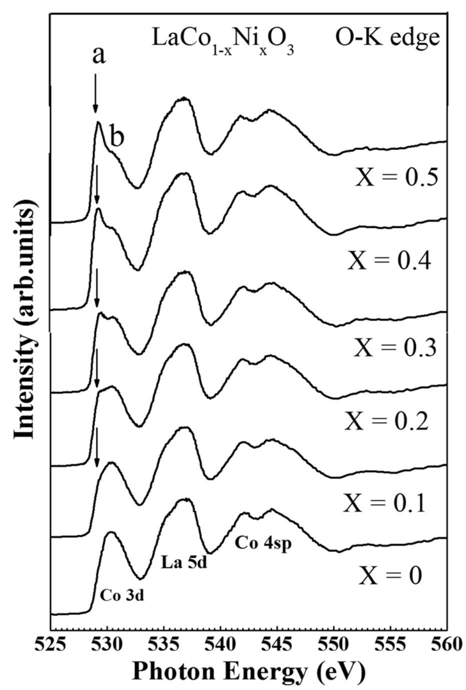


FIG. 5. XANES spectra for the O K-edge of $LaCo_{1-x}Ni_xO_3$ ($0 \le x \le 0.5$). The arrows depict the continuous increase in intensity of feature "a" and simultaneous decrease in that of "b" with substitution.

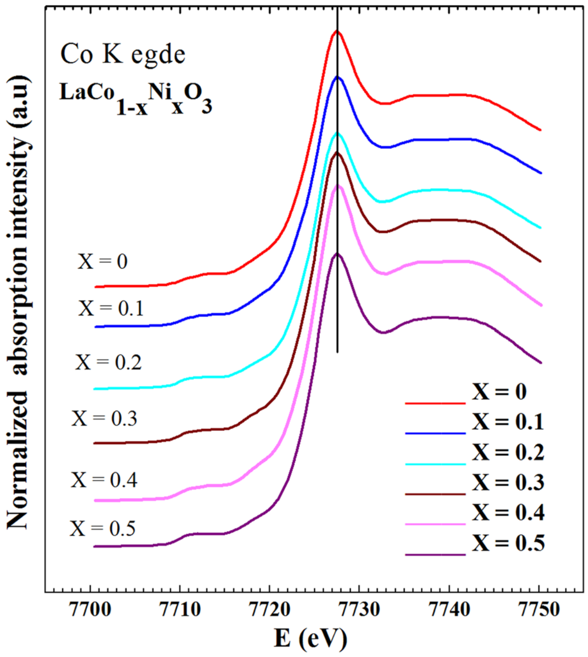


FIG. 6. XANES spectra for the Co K-edge of $LaCo_{1-x}Ni_xO_3$ ($0 \le x \le 0.5$). No edge shift observed indicating +3 valance state of Co in all compositions.

width. As a consequence, charge carriers find it easier to jump to the conduction band and the unoccupied density of states above the Fermi level shifted towards the Fermi level. This shifted density of states increases with increasing Ni content. These results are in accordance with the electrical transport results (see Sec. III B), where the resistance and activation energy progressively decreases with increase in the Ni substitution.

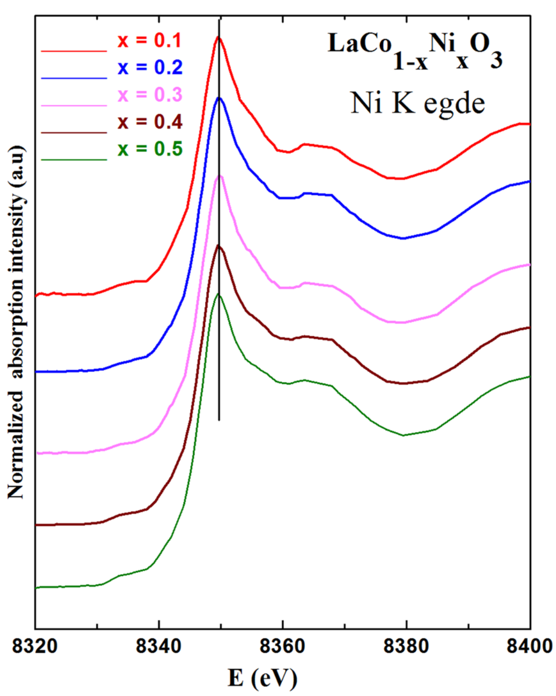


FIG. 7. XANES spectra for the Ni K-edge of $LaCo_{1-x}Ni_xO_3$ ($0.1 \le x \le 0.5$). No edge shift observed indicating +3 valance state of the Ni in all compositions.

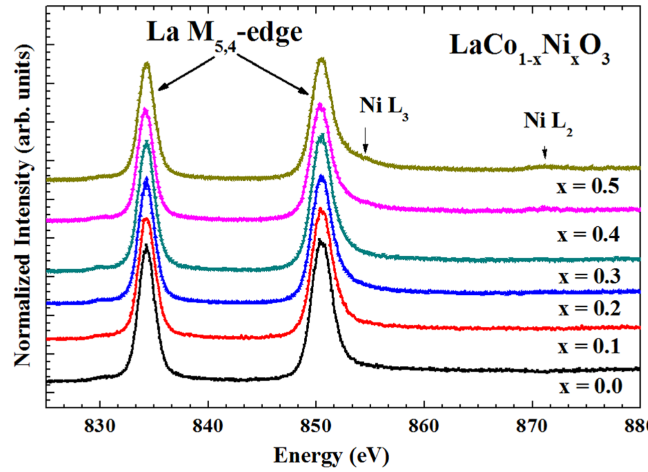


FIG. 8. XANES spectra at the La $M_{5,4}$ edge of $LaCo_{1-x}Ni_xO_3$ ($0.1 \le x \le 0.5$). Spectra confirm +3 valance state of La in all compositions.

Further to determine the valence state of the Co/Ni, we have measured XANES spectra at K-edge of Co and Ni (see Figs. 6 and 7), which confirms trivalent state for these ions in all the prepared compositions.[32,39–41] Also, La $M_{5,4}$-edge probes the unoccupied density of La 4*f* states and can give a clear indication of valence state of La. Figure 8 shows the $M_{5,4}$ edge of La, and we can see an overlap of La $M_4$ and Ni $L_3$-edges due to very small energy separation between La 3*d* and Ni 2*p* core levels, which is clearly visible in the spectra particularly that for $x = 0.4$, 0.5. However, the observed spectra of the pure as well as the substituted samples match well with that of $La^{+3}$ reported in the literature[42] indicating +3 charge state of La in all the prepared compositions. Thus, the XAS studies confirm the chemical state of each ion present in the system and also verify the homovalency of the substituted ions.

## IV. CONCLUSION

In summary, we have prepared the single phase $LaCo_{1-x}Ni_xO_3$ ($x \le x \le 0.5$) series by solid state reaction method. The structural analysis of samples confirms single phase rhombohedral structure with space-group $R\bar{3}c$. The electronic structure was studied using x-ray absorption near edge spectroscopy of the O, Co, Ni K-edge, and La $M_{5,4}$ edge. With Ni substitution, the O K-edge spectra show a feature about 1.2 eV lower than that of $LaCoO_3$. The intensity of this feature grows as the concentration of Ni increases. This is consistent with our resistivity data which show a systematic and fast decrease in resistivity with increase in the Ni content. Further XANES studies on K-edge of the Co/Ni and La $M_{5,4}$ edge confirm the trivalent state of the Co/Ni and La. The resistivity data have been fitted and analyzed with Arrhenius and ES type VRH model in different temperature ranges. The activation energy decreases and localization length increases systematically with the increase in Ni concentration. The observed features have been explained on the basis of increase in charge-carrier density with Ni substitution in $LaCoO_3$. The disorder-induced localization of charge carriers has been found to govern the conduction mechanism.

## ACKNOWLEDGMENTS

The authors would like to thank Roman Chernikov for the help during the XAS measurements at C beam line of the DORIS III storage ring (DESY, Hamburg, Germany).

[1]W. C. Koehler and E. O. Wollan, J. Phys. Chem. Solids **2**, 100 (1957).
[2]C. S. Naiman, R. Gilmore, B. Dibartolo, A. Linz, and R. Santoro, J. Appl. Phys. **36**, 1044 (1965).
[3]N. Menyuk, K. Dwight, and P. M. Raccah, J. Phys. Chem. Solids **28**, 549 (1967).
[4]A. Chainani, M. Mathew, and D. D. Sarma, Phys. Rev. B **46**, 9976 (1992).
[5]M. Abbate, J. C. Fuggle, A. Fujimori, L. H. Tjeng, C. T. Chen, R. Potze, G. A. Sawatzky, H. Eisaki, and S. Uchida, Phys. Rev. B **47**, 16124 (1993).
[6]S. Yamaguchi, Y. Okimoto, H. Taniguchi, and Y. Tokura, Phys. Rev. B **53**, R2926 (1996).
[7]M. A. Korotin, S. Y. Ezhov, I. V. Solovyev, V. I. Anisimov, D. I. Khomskii, and G. A. Sawatzky, Phys. Rev. B **54**, 5309 (1996).
[8]J. Hejtmánek, Z. Jirák, K. Knížek, M. Maryško, M. Veverka, and C. Autret, J. Magn. Magn. Mater. **320**, e92 (2008).
[9]Y. F. Zhang, S. Sasaki, O. Yanagisawa, and M. Izumi, J. Magn. Magn. Mater. **310**, 1002 (2007).
[10]X. G. Luo, X. Li, G. Y. Wang, G. Wu, and X. H. Chen, J. Solid State Chem. **179**, 2174 (2006).
[11]J. Dho and N. H. Hur, Solid State Communication **138**, 152–156 (2006).
[12]N. Y. Vasanthacharya, P. Ganguly, and J. B. Goodenough, J. Phys. C **17**, 2745 (1984).
[13]Y. Kobayashi, S. Murata, K. Asai, J. M. Tranquada, G. Shirane, and K. Kohn, J. Phys. Soc. Jpn. **68**, 1011 (1999).
[14]D. Hammer, J. Wu, and C. Leighton, Phys. Rev. B **69**, 134407 (2004).
[15]J. Androulakis, N. Katsarakis, and J. Giapintzakis, J. Appl. Phys. **91**, 9952 (2002).
[16]J. Androulakis, N. Katsarakis, Z. Viskadourakis, and J. Giapintzakis, J. Appl. Phys. **93**, 5484 (2003).
[17]T. Wu, G. Wu, and X. H. Chen, Solid State Commun. **145**, 293 (2008).
[18]V. Kumar, Y. Kumar, R. Kumar, D. K. Shukle, S. K. Arora, I. V. Shevet, and R. Kumar, J. Appl. Phys. **113**, 043918 (2013).
[19]D. D. Sarma, O. Rader, T. Kachel, A. Chainani, M. Mathew, K. Holldack, W. Gudat, and W. Eberhardt, Phys. Rev. B **49**, 14238 (1994).
[20]R. Kumar, R. J. Choudhary, M. Wasi Khan, J. P. Srivastava, C. W. Bao, H. M. Tsai, J. W. Chiou, K. Asokan, and W. F. Pong, J. Appl. Phys. **97**, 093526 (2005).
[21]B. Ravel and V. Newville, J. Synchrotron Radiat. **12**, 537 (2005).
[22]N. F. Mott and E. A. Davis, *Electronic Processes in Non-Crystalline Materials* (Clarendon Press, Oxford, 1971).
[23]A. L. Efros, *Electronic Properties of Doped Semiconductors* (Springer, 1984).
[24]A. K. Raydchaudhuri, Adv. Phys. **44**, 21 (1995).
[25]Spin Electronics, Lecture Notes in Physics, edited by M. J. Thornton and M. Ziese (Springer-Verlag, Berlin Heidelberg, 2001), pp. 89–116.
[26]T. Wolfram and S. Ellialtioglu, *Electronic and Optical Properties of D-Band Perovskites* (Cambridge University Press, New York, 2006).
[27]J. P. Cacho, J. Blasco, J. García, and J. Stankiewicz, Phys. Rev. B **59**, 14424 (1999).
[28]N. F. Mott, *Metal Insulator Transitions* (Taylor and Francis, London, 1990).
[29]P. W. Anderson, Phys. Rev. **109**, 1492 (1958).
[30]N. F. Mott, Philos. Mag. **19**, 835 (1969).
[31]N. F. Mott, Philos. Mag. **22**, 7 (1970).
[32]O. Toulemonde, N. N. Guyen, and F. Studer, J. Solid State Chem. **158**, 208 (2001).
[33]M. Medarde, A. Fontaine, J. L. García-Muñoz, J. Rodríguez-Carvajal, M. de Santis, M. Sacchi, G. Rossi, and P. Lacorre, Phys. Rev. B **46**, 14975 (1992).
[34]E. V. Tsipis, E. A. Kiselev, V. A. Kolotygin, J. C. Waerenborgh, V. A. Cherepanov, and V. V. Kharton, Solid State Ionics **179**, 2170 (2008).
[35]K. Iwasaki, T. Ito, M. Yoshino, T. Matsui, T. Nagasaki, and Y. Arita, J. Alloys Compd. **430**, 297 (2007).
[36]Z. Y. Wu, M. Benfatto, M. Pedio, R. Cimino, S. Mobilio, S. R. Barman, K. Maiti, and D. D. Sarma, Phys. Rev. B **56**, 2228 (1997).
[37]R. Kumar, R. J. Chaudhary, M. Ikram, D. K. Shukla, S. Mollah, P. Thakur, K. H. Chae, B. Angadi, and W. K. Choi, J. Appl. Phys. **102**, 073707 (2007).
[38]A. Bashir, M. Ikram, R. Kumar, P. Thakur, K. H. Chae, W. K. Choi, and V. R. Reddy, J. Phys.: Condens. Matter **21**, 325501 (2009).
[39]J. L. Hueso, J. P. Holgado, R. Pereniguez, S. Mun, M. Salmeron, and A. Caballero, J. Solid State Chem. **183**, 27 (2010).
[40]O. Haas, R. P. W. J. Struis, and J. M. McBreen, J. Solid State Chem. **177**, 1000 (2004).
[41]H. Y. Lee, T. B. Wu, and J. F. Lee, J. Appl. Phys. **80**, 2175 (1996).
[42]E. Benckiser, M. W. Haverkort, S. Bruck, E. Goering, S. Macke, A. Frano, X. Yang, O. K. Andersen, G. Cristiani, H. U. Habermeier, A. V. Boris, I. Zegkinoglou, P. Wochner, H. J. Kim, V. Hinkov, and B. Keim, Nature Mater. **10**, 189 (2011).